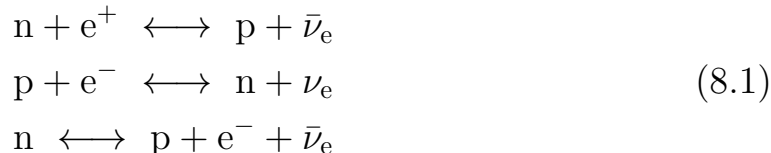


PRIMORDIAL NUCLEOSYNTHESIS

Our discussion at the end of the previous lecture concentrated on the relativistic components of the Universe, photons and leptons. Baryons (which are non-relativistic) did not figure because they make a trifling contribution to the energy density. However, from $t \sim 1$ s a number of nuclear reactions involving baryons took place. The end result of these reactions was to lock up most of the free neutrons into ${}^4\text{He}$ nuclei and to create trace amounts of D, ${}^3\text{He}$, ${}^7\text{Li}$ and ${}^7\text{Be}$. This is *Primordial Nucleosynthesis*, also referred to as Big Bang Nucleosynthesis (BBN).

8.1 The Neutron-to-Proton Ratio

Before neutrino decoupling at around 1 MeV, neutrons and protons are kept in mutual thermal equilibrium through charged-current weak interactions:



While equilibrium persists, the relative number densities of neutrons and protons are given by a Boltzmann factor based on their mass difference:

$$\left(\frac{n}{p}\right)_{\text{eq}} = \exp\left[-\frac{\Delta m c^2}{kT}\right] = \exp\left[-\frac{1.5}{T_{10}}\right] \tag{8.2}$$

where

$$\Delta m = (m_n - m_p) = 1.29 \text{ MeV} = 1.5 \times 10^{10} \text{ K} \tag{8.3}$$

and T_{10} is the temperature in units of 10^{10} K.

As discussed in Lecture 7.1.2, this equilibrium will be maintained so long as the timescale for the weak interactions is short compared with the timescale of the cosmic expansion (which increases the mean distance between particles). In 7.2.1 we saw that the ratio of the two rates varies approximately as:

$$\frac{\Gamma}{H} \simeq \left(\frac{T}{1.6 \times 10^{10} \text{ K}}\right)^3. \tag{8.4}$$

This steep dependence on temperature can be appreciated as follows. We have already encountered many times the expression for the Hubble parameter as a function of redshift:

$$\frac{H(z)}{H_0} = \sqrt{\Omega_{\text{m},0}(1+z)^3 + \Omega_{\text{rad},0}(1+z)^4 + \Omega_{\text{k},0}(1+z)^2 + \Omega_{\Lambda,0}} \quad (8.5)$$

from which we see that in the radiation dominated era the expansion rate is proportional to the square root of the energy density in radiation, which in turn is proportional to T^4 (eq. 7.28). Thus, $H \propto T^2$.

On the other hand, the rate per neutron of the reactions at eq. 8.1 is proportional to (i) the number of electron neutrinos, $n(\nu_e, \bar{\nu}_e)$, and (ii) the weak interaction cross-section $\langle\sigma\rangle$. In turn, $\langle\sigma\rangle$ is proportional to (i) T^2 , and (ii) the reciprocal of the neutron half-life for free decay, $\tau_{1/2}^{-1}$, which measures the intrinsic strength of the interaction. Since $n(\nu_e, \bar{\nu}_e) \propto T^3$, $\Gamma \propto T^5$, and hence $\Gamma/H \propto T^3$.

As T decreases, there comes a point at

$$kT_{\text{d}} \approx 0.8\text{MeV} = (m_{\text{n}} - m_{\text{p}}) - m_{\text{e}}$$

where the weak interaction rate falls rather suddenly below the expansion rate and the ratio n/p is frozen (apart from free decay and some residual weak interactions). Thus, at $t \simeq 2.6$ s, $T_{\text{d}} \simeq 0.8$ MeV (the **neutron freeze-out**), the ratio n/p is:

$$\frac{\text{n}}{\text{p}} = \exp\left[-\frac{\Delta m c^2}{kT_{\text{d}}}\right] = \exp\left[-\frac{1.3}{0.8}\right] = 0.20 = 1 : 5 \quad (8.6)$$

The precise value of the decoupling temperature T_{d} depends on the two physical constants \mathcal{N}_{ν} and $\tau_{1/2}$:

$$T_{\text{d}}^3 \propto \tau_{1/2} \left(\frac{11}{4} + \frac{7}{8}\mathcal{N}_{\nu}\right)^{1/2}; \quad (8.7)$$

implying that larger values of either of these constants lead to higher T_{d} , higher n/p, and therefore a higher primordial abundance of ${}^4\text{He}$, given that essentially all of the available neutrons are later incorporated into ${}^4\text{He}$ nuclei, as we shall see in a moment.

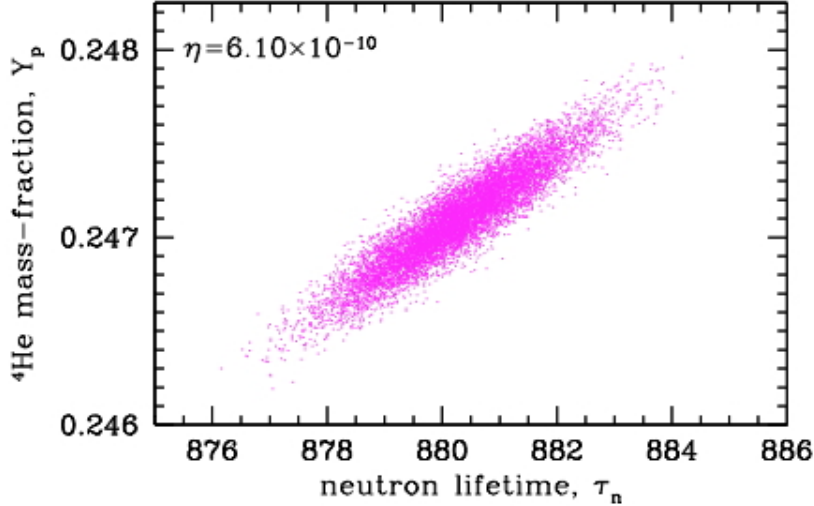
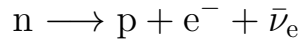


Figure 8.1: Dependence of the primordial abundance of ${}^4\text{He}$ by mass, Y_p , on the value of the neutron mean life, τ_n (s), from the error propagation calculations by Cyburt et al. (2015).

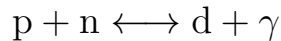
8.2 Deuterium Formation

After neutron freeze-out the only reaction that appreciably changes the number of neutrons is neutron decay:



with a mean life $\tau_n = 880.3 \pm 1.1$.¹

Without further reactions to preserve neutrons within stable nuclei, the Universe today would be essentially pure hydrogen. The reaction that preserves neutrons is deuteron formation (deuteron is the nucleus of deuterium, the simplest isotope of hydrogen):



This reaction is exothermic, with an energy difference of 2.225 MeV (the binding energy of the D nucleus, E_D). Since the strong interaction is at play here, the formation of D proceeds very efficiently. However, the temperature at $t \sim$ a few seconds is not much lower than 2.2 MeV and, given that photons are a billion times more numerous than baryons (see eq. 7.6), there are sufficient photons with energies $E_\gamma > E_D$ in the Wien tail of the blackbody distribution to instantly destroy newly formed D

¹In general, for radioactive decays $N(t) = N_0 e^{-\lambda t}$, where the decay constant $\lambda \equiv 1/\tau$, and the half-life $t_{1/2} = \tau \ln 2$.

by photo-dissociation. We thus have to wait until the temperature has fallen sufficiently for a substantial concentration of D to build up before primordial nucleosynthesis can get going in earnest. This is sometimes referred to as the *Deuterium bottleneck*.

Consideration of the relevant balance equations shows that the formation rate of D exceeds its photo-dissociation rate at $T_D \simeq 8 \times 10^8$ K. This is attained at time $t \sim 300$ s, at which point the ratio n/p has fallen from the value at eq. 8.6 by a factor $\exp[-300/(880.3)] = 0.71$ to $n/p = 0.14$ or 1:7.

This ratio immediately gives us an approximate estimate of the primordial helium mass fraction, Y_p , because virtually all neutrons surviving after 300 s are later incorporated into ${}^4\text{He}$. Thus:

$$Y_p = \frac{4 \frac{n}{2}}{p + n} = \frac{2n}{p + n} = \frac{2 \frac{n}{p}}{1 + \frac{n}{p}} = 0.25 \quad (8.8)$$

which corresponds to a ratio ${}^4\text{He}/\text{H} = 1/12$ by number (since a ${}^4\text{He}$ nucleus weighs four times as much as H).

It is a coincidence that the neutron mean life is so comparable to the time it takes for nuclei to form; if it were much shorter, all the neutrons would have decayed before primordial nucleosynthesis had had a chance to proceed and only hydrogen would remain.

8.3 Nuclear Reactions

Once the d/p ratio has built up to $\sim 10^{-5}$, further reactions proceed to synthesize helium and other light nuclei. The most important reactions are collected in Figure 8.2.

As already mentioned, ${}^4\text{He}$ soaks up virtually all of the neutrons available. After the formation of ${}^4\text{He}$, traces amounts D and ${}^3\text{He}$ survive because nuclear reactions are frozen out by low density and temperature before their destruction is complete. Still smaller traces of ${}^7\text{Li}$ and ${}^7\text{Be}$ (which later decays to ${}^7\text{Li}$) are formed and survive. The outcome of primordial nucleosynthesis is calculated by numerically following the series of relevant nuclear reactions shown in Figure 8.2; Figure 8.3 shows the progress of BBN with time.

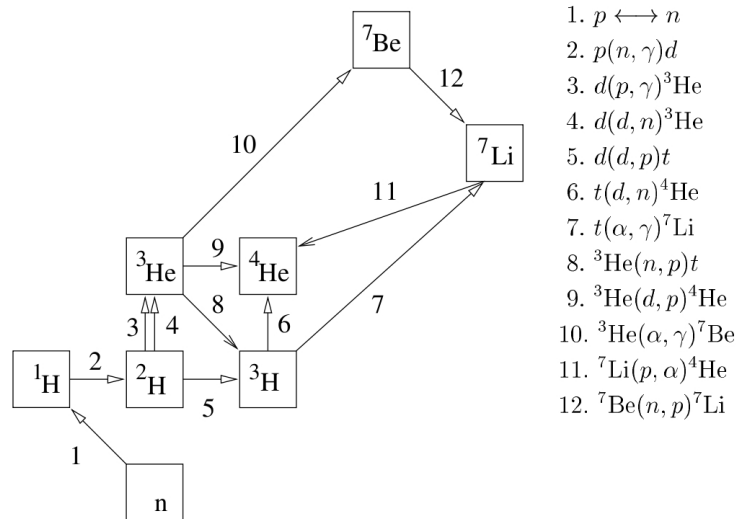


Figure 8.2: The network of reactions for Big Bang nucleosynthesis (from Nollett & Burles 2000). *Key:* $p(n, \gamma)d \equiv p + n \rightarrow d + \gamma$.

BBN stops at ^7Li because no stable nucleus of mass number 5 or 8 exists and thus no new nuclei can be formed in collisions of two He nuclei or a proton with a He nucleus. Collisions between three nuclei are far too rare to contribute. The important point here that how far the BBN nuclear reactions in Figure 8.2 proceed before they are frozen out by low density and temperature depends on the parameter $\eta \equiv n_b/n_\gamma$ which we have already encountered in Lecture 7. As explained there, η is related to the

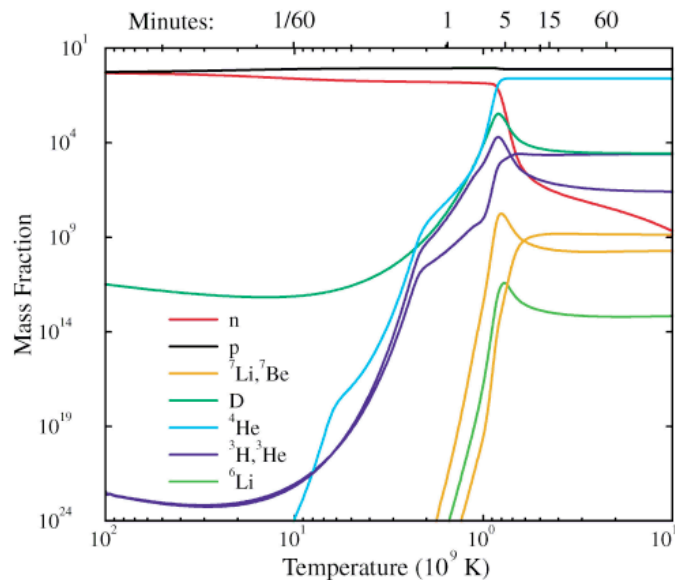


Figure 8.3: Fractional abundances of the light elements produced in BBN as a function of time and temperature. Note that the minus sign in the exponent of the units on the y -axis appears to have been lost in the reproduction of this figure.

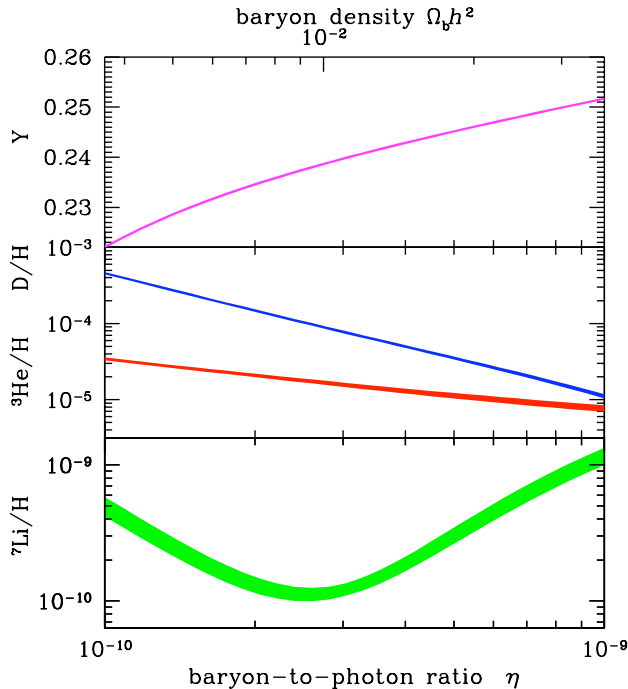


Figure 8.4: The abundances of light elements relative to H predicted by BBN calculations are shown as functions of $\eta \equiv n_b/n_\gamma$ (bottom x -axis) and $\Omega_{b,0}h^2$ (top x -axis). It is customary to express the primordial abundance of ${}^4\text{He}$ *by mass* (Y_p), and those of the other elements *by number*. The widths of the curves reflect the uncertainties in the predictions, propagated from uncertainties in the experimental values of the relevant nuclear reaction rates. (Figure reproduced from Cyburt et al. 2015).

cosmic density of baryons in units of the critical density, $\Omega_{b,0}h^2$ via the temperature of the cosmic microwave background today, $T_{\gamma,0}$:

$$\eta_{10} = 273.3 \Omega_{b,0}h^2 \left(\frac{2.7255 \text{ K}}{T_{\gamma,0}} \right)^3 \quad (8.9)$$

where η_{10} is $10^{10}\eta$. Figure 8.4 illustrates the dependence on η and $\Omega_{b,0}h^2$ of the relative abundances of the light elements produced in BBN.

It is worthwhile considering the following aspects of Figure 8.4:

- Y_p has a very minor dependence on η because, as we have explained, essentially all of the neutrons end up in ${}^4\text{He}$. For larger baryon-to-photon ratios, the balance between D formation and photo-dissociation moves to slightly larger values of T_D (i.e. the deuterium bottleneck does not last as long; see section 8.2). The earlier D can form, the fewer neutrons have decayed, and hence Y_p is slightly larger.
- In a similar vein, the higher η , the more efficient is the conversion of D into ${}^4\text{He}$ which proceeds via two-body reactions with p, n, D, and ${}^3\text{He}$

(see Figure 8.2). This leads to the steep inverse dependence of $(D/H)_p$ on η in Figure 8.4. ${}^3\text{He}$ declines more gently because this nucleus is more robust.

- ${}^7\text{Li}$ has a bimodal behaviour because it can be produced via two channels, labelled 10 and 7 in Figure 8.2. Reaction 7 is favoured at low baryon densities, while 10 takes over at high values of η .

8.4 Measures of Primordial Abundances of the Light Elements

The remarkable implication of Figure 8.4 is that, by measuring the primordial abundance of one of the light elements created in BBN, it is possible to literally ‘weigh’ the Universe, at least in baryons. Measurement of two or more elements would in addition allow us to test the theory, since the values of η indicated by any two elements should agree. In this section, we shall consider the experimental verification of BBN predictions.

Before we start, we should make clear a few key facts. The relative abundances of the light elements created in BBN remained unaltered for the first ~ 200 Myr.² However, once the first stars formed at $z \sim 20$, the BBN abundances began to be changed by the process of galactic chemical evolution. All of the elements of the periodic table heavier than Boron were synthesised in the interiors of stars and some fraction of these was returned to the interstellar medium to be incorporated in successive stellar generations. Thus, as time progressed, the ‘metal’ content of the Universe steadily increased (astronomers use the terms ‘metals’ and ‘metallicity’ to refer to all elements with atomic number 6 or greater—that is C and heavier elements—that were created exclusively by stellar nucleosynthesis).

Since we cannot view the Universe directly at the early times when BBN took place or soon after, the determination of the primordial abundances of the light elements is based on identifying astrophysical environments—whether galaxies, gas clouds or stars—that have undergone minimum enrichment by stellar nucleosynthesis. Determination of ${}^4\text{He}/\text{H}$, D/H , ${}^7\text{Li}/\text{H}$ in such ‘low metallicity’ environments can then lead to these elements’ pri-

²With the exception of ${}^7\text{Be}$ which swiftly decays to ${}^7\text{Li}$, but only once the Universe has cooled sufficiently for the ${}^7\text{Be}$ nucleon to capture an electron.

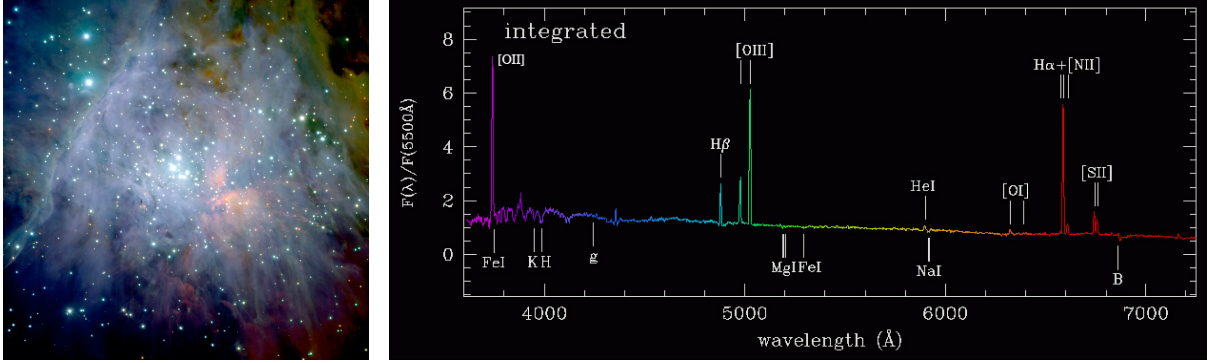


Figure 8.5: *Left:* Near-IR image of the central part of the Orion nebula, obtained with the Very Large Telescope of the European Southern Observatory. The nebula is diffuse gas ionised by hot stars. *Right:* Typical emission line spectrum of an H II region such as the Orion Nebula. The most important spectral features are labelled.

mordial abundances, sometimes with appropriate corrections/extrapolations to zero metallicity. Note that we have not included ^3He in the above list. This isotope has so far been detected only in the the Milky Way interstellar medium, which is far from being a pristine environment, and correcting for its post-BBN history is too uncertain for ^3He to be a useful probe of BBN.

We now discuss the most recent determinations of Y_p , $(\text{D}/\text{H})_p$, and $(^7\text{Li}/\text{H})_p$. For practical reasons, each of these ratios is most easily accessed in a different astrophysical environment.

8.4.1 $^4\text{Helium}$

The abundance of ^4He has been measured for decades from the emission line spectra of H II regions, volumes of the interstellar medium ionised by the ultraviolet radiation of massive, short-lived stars. Our closest H II region is the Orion nebula, visible with the naked eye from northern latitudes in winter months (see Figure 8.5).

^4He is created by the fusion of 4 H nuclei in the hot cores of stars; thus its abundance *increases* over the primordial value (which should provide a universal ‘floor’) as interstellar gas is cycled through successive episodes of star formation.

In the local Universe, there is a well-established relationship between the mass of a galaxy and its metallicity: the least massive galaxies are also the ones with the lowest fraction of metals, either because they have not turned a significant fraction of their gas into stars, or because they cannot retain

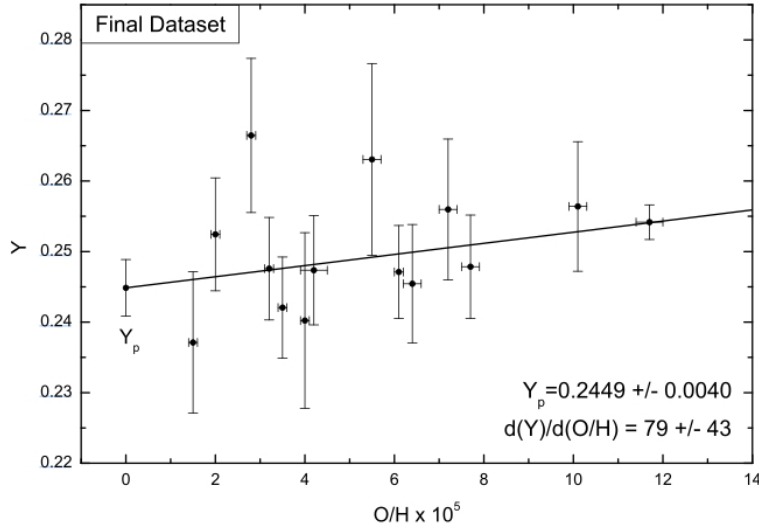


Figure 8.6: The abundance of ${}^4\text{He}$ by mass in the lowest metallicity dwarf galaxies known, plotted as a function of the O abundance. For comparison, in the Sun, in the Orion nebula, and generally in the Milky Way galaxy $(\text{O}/\text{H})_{\odot} \simeq 5 \times 10^{-4}$; thus, the galaxies with the lowest O abundance in this figure have $(\text{O}/\text{H}) \simeq 0.04 (\text{O}/\text{H})_{\odot}$. The authors of this study (Aver et al.2015) find a shallow gradient in the regression of Y with (O/H) : $d(Y)/d(\text{O}/\text{H}) = 79 \pm 43$ and deduce $Y_{\text{p}} = 0.245 \pm 0.004$. However, a zero gradient would be an almost equally good fit to the data. This illustrates one of the uncertainties in the determination of the *primordial* value of Y .

the products of stellar nucleosynthesis in their shallow potential wells (or both). Thus, efforts to determine Y_{p} have focussed on measuring the ratio ${}^4\text{He}/\text{H}$ from the emission lines of H II regions in the lowest mass (dwarf), most-metal-poor galaxies known.

As can be seen from Figure 8.6, the current best estimate $Y_{\text{p}} = 0.245 \pm 0.004$ is in excellent agreement with BBN predictions (eq. 8.8). This is strong empirical evidence that the basic idea of a hot Big Bang is correct.³

It can also be appreciated from Figure 8.4 that Y_{p} is not a sensitive measure of η and $\Omega_{\text{b},0}$: Y_{p} increases by only $\sim 15\%$ from $Y_{\text{p}} = 0.220$ to 0.252 as η varies by one order of magnitude, from $\eta = 10^{-10}$ to 10^{-9} . It can be difficult to achieve precisions of a few percent in astrophysical measurements, usually because all the sources of systematic error are hard to identify and correct for. The determination of the He abundance in H II regions is a case in point, with many factors contributing uncertainties of a few percent. The extrapolation from the values of Y measured in metal-poor galaxies to the

³As a historical note, the fact that there is a floor to the He abundance at $Y_{\text{p}} \simeq 0.25$ was beginning to be realised at the end of the 1940s and it led to the conjecture that (some) chemical elements may have been synthesised in the early Universe.

primordial value adds a further layer of uncertainty (see Figure 8.6). For all of these reasons, even the most careful analyses return an error which is still frustratingly larger than required to pin down $\Omega_{\text{b},0}$. The conclusion by Aver et al. (2015) that $Y_{\text{p}} = 0.245 \pm 0.004$ translates to $\Omega_{\text{b},0}h^2$ values between $\sim 8 \times 10^{-3}$ and $\sim 2.7 \times 10^{-2}$, or $0.018 \leq \Omega_{\text{b},0} \leq 0.059$ for $h = 0.675$ (from now on we shall quote values of $\Omega_{\text{b},0}$ which assume $h = 0.675$). Note that even the upper limit immediately tells us that baryons only account for a few percent of the critical density.

8.4.2 Deuterium

While less abundant than ${}^4\text{He}$ by two-to-four orders of magnitude, D is a far more sensitive ‘*baryometer*’, given its steep inverse dependence on η (Figure 8.4). Unlike He, the fragile D is burnt in the late stages of star formation; thus, over the cosmic ages the ratio D/H has decreased from its primordial value—a process referred to as the ‘*astration*’ of deuterium. Consequently, measurements of D/H in the interstellar gas of the Milky Way provide an upper limit to $\Omega_{\text{b},0}$.

$(\text{D}/\text{H})_{\text{p}}$ is deduced from the analysis of absorption lines in pockets of interstellar gas at high redshift which has undergone minimum processing through stars, as indicated by its low metallicity ($Z_{\text{gas}} < 1/100Z_{\odot}$). As we shall see in subsequent lectures, the spectra of high redshift sources (mostly quasars) show a multitude of absorption lines at different redshifts, produced by intervening hydrogen gas in galaxies and between galaxies. Each of these H I absorption lines has a component due to D, blueshifted by 82 km s^{-1} as a result of the slightly higher energy levels of the D atom compared to H.

Normally, the D I component cannot be separated from the stronger H I absorption, or is too weak to be detected at all, but in a few, rare cases where all the required conditions are met,⁴ it has proved possible to measure $(\text{D}/\text{H})_{\text{p}}$ with high precision (see Figure 8.7). The value $(\text{D}/\text{H})_{\text{p}} = (2.527 \pm 0.030) \times 10^{-5}$ reported by Cooke et al. (2017) implies $\Omega_{\text{b},0} = (4.91 \pm 0.11) \times 10^{-2}$ (both random and systematic errors are included). This value is consistent with, and much more precise than, the value of

⁴These include low velocity dispersion, high column density, low metallicity and convenient redshift of the absorbing gas, and high luminosity of the background quasar.

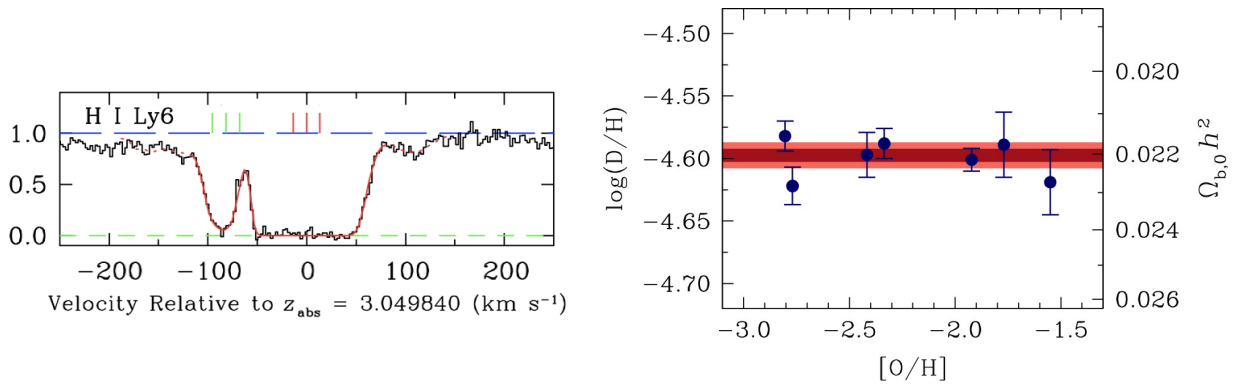


Figure 8.7: *Left:* The D I component is clearly resolved at $v = -82 \text{ km s}^{-1}$ in the transition from the $n = 1$ to the $n = 7$ energy level of H I seen in absorption against the quasar J1419+0829. *Right:* The seven high-precision determinations of (D/H) from quasar absorption line spectroscopy. The dark and light red bands show the 1 and 2 σ confidence limits on $(D/H)_p$. Figures adapted from Cooke et al. (2014, 2017).

$\Omega_{b,0}$ deduced from Y_p (section 8.4.1).

8.4.3 ${}^7\text{Lithium}$

${}^7\text{Li}$ is most easily observed in the atmospheres of cool stars, via a pair of weak absorption lines of Li I at $\lambda\lambda 6707.76, 6707.91$. The post-BBN evolution of the Li abundance is complex; ${}^7\text{Li}$ is both synthesised and destroyed during the lifetime of stars, and in addition can be produced by the interaction of high energy cosmic rays with atoms in the Galactic ISM. For this reason, astronomers have looked preferentially at the oldest stars, which are located in the halo of the Milky Way, with the hope of finding a floor in the values of ${}^7\text{Li}/\text{H}$ indicative of $({}^7\text{Li}/\text{H})_p$.

Indeed, such a plateau was discovered in the early 1980s: stars with iron abundance $-3 \leq [\text{Fe}/\text{H}] \leq -1.5$ ⁵ have $({}^7\text{Li}/\text{H}) = (1.6 \pm 0.3) \times 10^{-10}$. The lack of significant dispersion about this value led to the suggestion that it may indeed represent the primordial abundance of ${}^7\text{Li}$.

However, this interpretation has now come into question for two reasons: (1) The plateau does not continue to lower metallicities—stars with $[\text{Fe}/\text{H}] < -3$ have even lower values of ${}^7\text{Li}/\text{H}$ (see Figure 8.8); and (2) The plateau value, $({}^7\text{Li}/\text{H}) = (1.6 \pm 0.3) \times 10^{-10}$ is ~ 3 times lower than the value predicted by BBN calculations if $\Omega_{b,0} = (4.83 \pm 0.10) \times 10^{-2}$, as deduced from deuterium (see Figure 8.9). To date, the ‘Li problem’ remains unsolved. It is unclear whether its solution will come from a better understanding

⁵This is a convenient shorthand notation: $[\text{Fe}/\text{H}] \equiv \log(\text{Fe}/\text{H})_{\text{star}} - \log(\text{Fe}/\text{H})_{\odot}$.

of physical processes in the interiors of stars, or a revision of the relevant network of nuclear reactions.

8.5 Dark Matter

Anticipating some of the material in the next lectures, a completely independent determination of $\Omega_{b,0}h^2$ is arrived at from the analysis of the power spectrum of temperature fluctuations of the cosmic microwave background. The latest, and most accurate, measure is from the *Planck* mission of the European Space Agency which yielded $\Omega_{b,0}h^2 = (2.226 \pm 0.023) \times 10^{-2}$, or $\Omega_{b,0} = (4.886 \pm 0.050) \times 10^{-2}$ for $h = 0.675$. As can be seen from Figure 8.9, the CMB value is in spectacular agreement with that deduced from analysis of the D I absorption lines, giving us additional confidence in the hot Big Bang model of the Universe.

Thus, it now seems a secure statement that baryons contribute less than 5% of the critical density to the ‘Cosmic Inventory’ of Table 1.1. This leaves us with both a non-baryonic and a baryonic dark matter ‘problem’.

By non-baryonic dark matter we mean some component of the Universe which does not interact with photons, and therefore does not absorb nor emit light. This component interacts with ordinary matter (baryons) only through gravity, and indeed its existence is surmised from observations that

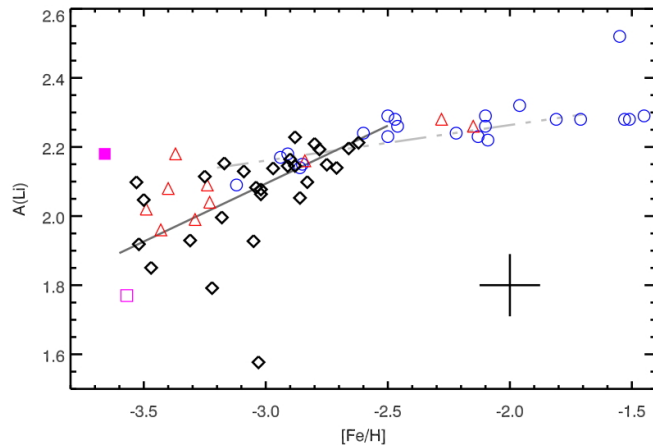


Figure 8.8: A collection of ${}^7\text{Li}$ abundance measurements in metal-poor halo stars, from Sbordone et al. (2010). The different symbols refer to different data sets brought together here. Typical errors are indicated by the black cross. The Li abundance scale (y -axis) is defined as $A(\text{Li}) \equiv \log(\text{Li}/\text{H}) + 12$.

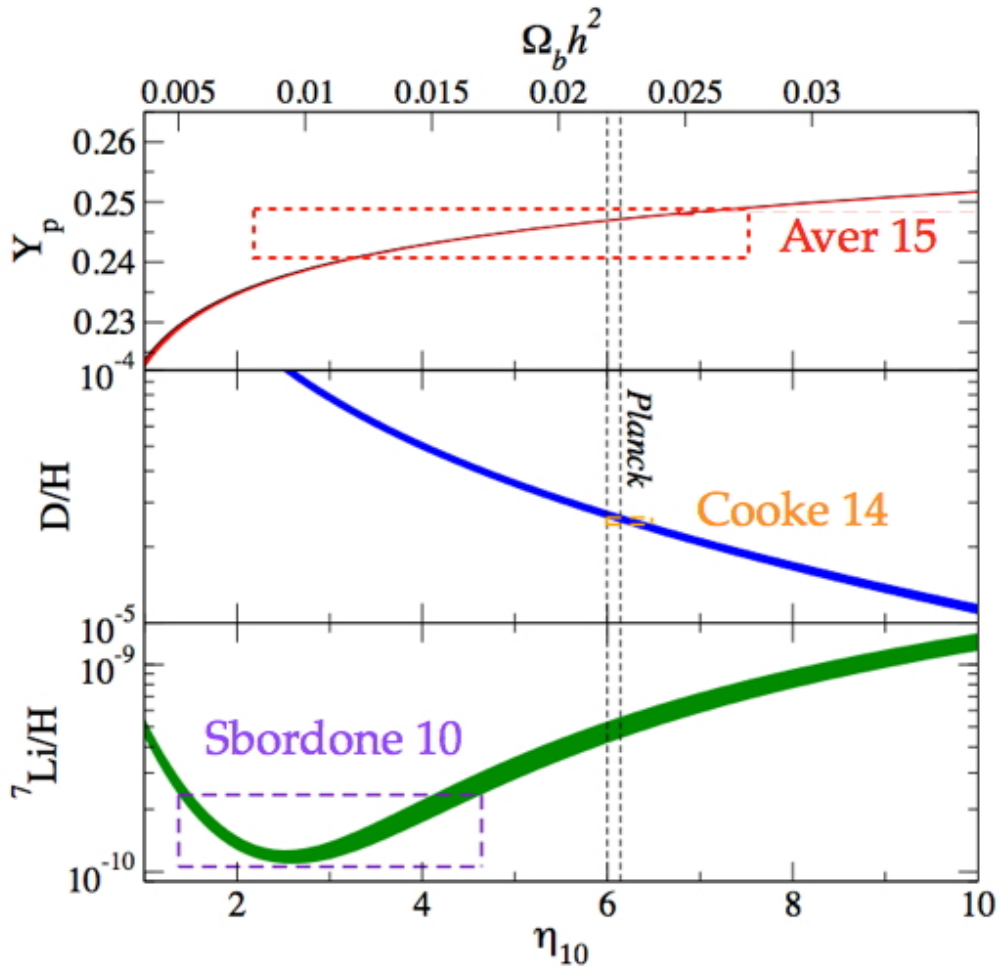


Figure 8.9: BBN theory confronts observations 2015 (adapted from Ichimasa et al. 2014).

ultimately involve gravity, such as the rotation curves of spiral galaxies (Lecture 1.6), the velocity dispersion of galaxies in groups and clusters, the growth of large scale structure in the distribution of galaxies, and gravitational lensing— all of these topics will be considered in subsequent lectures.

Again, it is the analysis of the CMB fluctuations that gives us the most accurate estimate: $\Omega_{m,0} = 0.312 \pm 0.009$, indicating that baryons account for only $\sim 15\%$ of the total matter in the Universe. The nature of non-baryonic dark matter remains a mystery and many searches are underway in underground laboratories and in particle accelerators to identify the presumably massive particle(s) responsible.

The term baryonic dark matter, on the other hand, is intended to simply point to a shortcoming in our accounting of the baryons in the Universe.

From consideration of the mass-to-light ratio, it is estimated that stars (and their remnants) and gas in galaxies contribute a trifling $\Omega_{\text{stars},0} \sim 0.003$ to the critical density. Presumably the remaining $\sim 94\%$ of the baryons are in gas in the halos of galaxies and in between galaxies (the intergalactic medium) that it is difficult to detect perhaps because it is of low density and/or at high temperature. Later on in the course we shall see that indeed a significant fraction of the baryons is accounted for by the intergalactic absorption lines found in the spectra of distant quasars at high redshifts.

8.6 Beyond the Standard Model?

Big-Bang nucleosynthesis is a topic at the interface between astrophysics and particle physics. One example of this close relationship is the neutron mean life, τ_n , which determines the value of Y_p (see Figure 8.1). In the 1980s, the He abundance in metal-poor nebulae was used to place constraints on τ_n , a quantity which is not straightforward to measure in the laboratory.

We have already seen in the preceding section that the existence of non-baryonic dark matter implied by the finding that $\Omega_{b,0} \simeq 1/6 \Omega_{m,0}$ requires an extension of the standard model of particle physics. If we must have dark matter, can we also have dark radiation? This term is meant to refer to any relativistic component of the Universe which is not accounted by the standard model.

If such a component existed and contributed to the thermal bath at the time of BBN, it would increase the effective number of degrees of freedom g_* in eq. 7.26 that determines the total energy density:

$$u = \frac{1}{2} g_* a T^4 = a T^4 \left[1 + \frac{7}{4} + \frac{7}{8} \mathcal{N}_\nu \right] \quad (8.10)$$

where \mathcal{N}_ν is the number of neutrino families.

The possible existence of an unrecognised relativistic component is often incorporated into the parameter \mathcal{N}_ν . We saw in eq. 8.7 that \mathcal{N}_ν determines the temperature of neutron freeze-out, and therefore the n/p ratio. It follows that one can use the observed abundances of the light elements to place constraints on the value of \mathcal{N}_ν . Figure 8.10 (left) shows that altering

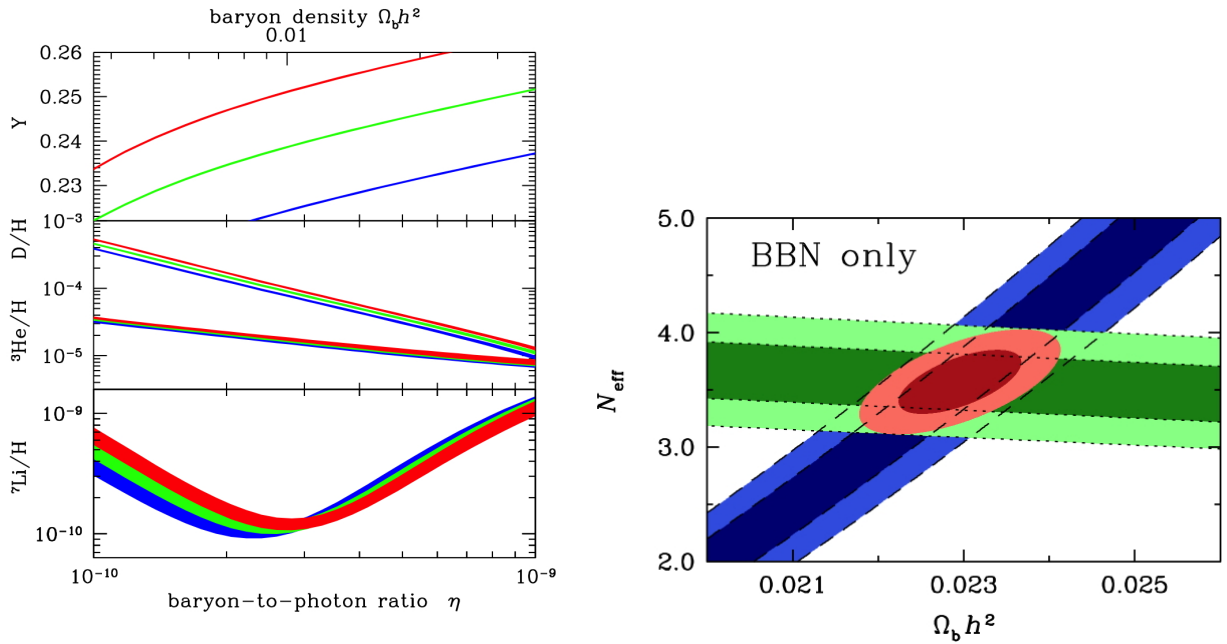


Figure 8.10: *Left:* BBN predictions for light element abundances for $\mathcal{N}_\nu = 4$ (red), 3 (green) and 2 (blue) from Cyburt et al. (2015). *Right:* Joint 1σ (darker colours) and 2σ (lighter colours) confidence contours for \mathcal{N}_ν and $\Omega_{b,0}$ obtained from the measured values of Y_p and $(D/H)_p$ (from Cooke et al. (2014)).

\mathcal{N}_ν has a large effect on the predicted value of Y_p (as expected); the impact on the abundances of the other light elements is smaller but detectable.

When the most recent empirical determinations of Y_p and $(D/H)_p$ discussed above (sections 8.4.1 and 8.4.2) are analysed together, they yield $\mathcal{N}_\nu = 2.85 \pm 0.28$ (Cyburt et al. 2015). The tighter limit, $\mathcal{N}_\nu = 2.88 \pm 0.16$ is obtained by combining BBN with the CMB. Thus, there is no evidence at the moment for a significant departure from the standard model value $\mathcal{N}_\nu = 3$. For comparison, the width of Z-boson decays in electron-positron colliders implies $\mathcal{N}_\nu = 2.984 \pm 0.008$ (ALEPH Collaboration 2006).

8.7 Summary

In this lecture we have seen how the simple consideration that the temperature of the cosmic background radiation increases as $T(z) = 2.7255(1+z)$ K leads us to conclude that there must have been an epoch in the early Universe when, over the course of a few minutes, the lightest elements of the periodic table were synthesised from protons and neutrons via a chain of

nuclear reactions whose rates can be measured in the laboratory today.

BBN makes the first-order prediction that ${}^4\text{He}$ accounts for approximately 25% of the mass in baryons, as indeed observed in the least polluted environments where the abundance of He can be measured. Recent measurements of the primordial abundance of deuterium strengthen the case further. While the ‘Li problem’ remains a thorn in the side, we feel justified in concluding that BBN is one of the pillars of the hot Big Bang model of the Universe.

Together with inferences drawn from the analysis of the CMB, it is now clear that baryons, the ordinary matter of our world, makes up just a little less than 5% of the cosmic mass-energy budget, and only about 15% of the cosmic density of matter. This opens the door to an unknown component of the Universe, Dark Matter, whose existence is primarily deduced from the gravity it exerts on the baryons, and in the bending of light rays in gravitational lensing. We have no idea of the masses or other physical properties of the particles making up the Dark Matter and how they might fit in the standard model of particle physics which includes quarks, lepton and gauge bosons. Interestingly, the existence of an analogous dark relativistic component seems excluded by: (a) the internal consistency of measures Y_p and $(\text{D}/\text{H})_p$, and (b) the good agreement between BBN and CMB determinations of $\Omega_{b,0}$.